

Contents lists available at [ScienceDirect](https://www.sciencedirect.com)

Comparative Biochemistry and Physiology, Part B

journal homepage: www.elsevier.com/locate/cbpb

Molecular characterization of *Pax7* and its role in melanin synthesis in *Crassostrea gigas*

Zhuanzhuan Li^a, Qi Li^{a,b,*}, Chengxun Xu^a, Hong Yu^a

^a Key Laboratory of Mariculture, Ministry of Education, Ocean University of China, Qingdao 266003, China

^b Laboratory for Marine Fisheries Science and Food Production Processes, Qingdao National Laboratory for Marine Science and Technology, Qingdao 266237, China

ARTICLE INFO

Editor: Chris Moyes

Keywords:

Pax7
Melanin synthesis
RNA interference
Crassostrea gigas

ABSTRACT

The paired-box 7 (*Pax7*) is a transcription factor crucial for skin color polymorphism. However, the mechanism underlying the pigmentation associated with *Pax7* in mollusks have yet to be elucidated. In this study, the cDNA sequence of *Pax7* in the Pacific oyster *Crassostrea gigas* (*CgPax7*) was characterized. Phylogenetically, the identity of deduced amino acid sequence was similar to that of other mollusks and contained 463 amino acids, with conserved features of paired domain (PRD), homeobox domain (HD) and octapeptide. Gene expression analysis revealed that *CgPax7* was markedly increased at D-shaped larvae stage and ubiquitously expressed in six examined tissues in adult oyster. The result of whole-mount in situ hybridization (WMISH) showed a restricted pattern of *CgPax7* expression on margins of shell valves at D-shaped and umbo larvae stages. Additionally, although *CgPax7* silencing had no significant effect on *CgMitf* expression, it significantly inhibited the expressions of *CgPax7*, *CgTyr*, *CgTypr1*, *CgTypr2* and *CgCdk2*, genes involved in Tyr-mediated melanin synthesis. Furthermore, *CgPax7* knockdown obviously decreased the tyrosinase activity. Less brown-granules at mantle edge was detected by micrographic examination and melanosomes defect was observed by transmission electron microscopy. It was demonstrated that *CgPax7* play a key role in melanin synthesis by regulating Tyr-pathway in *C. gigas*. These findings indicated the potential framework by which mollusks pigmentation.

1. Introduction

Melanin has attracted considerable interest because of their involvement in pigmentation and protection against ultraviolet (Ito et al., 2013). One of the widely-believed melanin synthesis pathway, wnt pathway, where PAX3 partnering with SOX10 induced the expression of *Mitf* and affected the expression of *Tyr*. Arguably, *Mitf*, a master regulator of melanogenesis, activates the expression of other melanocytes differentiation and migration related proteins, such as tyrosinase gene family, including *Tyr*, *Typr1*, and *Typr2* (Fang et al., 2001; Hartman and Czyz, 2015). TYR, catalyzing the rate-limiting step in melanogenesis, is a membrane-bound enzyme located on the melanosome, which catalyzes the oxidation of tyrosine to CRE (Land et al., 2004; Schallreuter et al., 2008). Dopaquinone is then converted to melanin polymer by TYRP1 and TYRP2 (Del Marmol and Beermann, 1996). In addition,

Typr1 gene also plays a role in survival and proliferation of melanocytes (Bian et al., 2021). However, the molecular pathway for melanin synthesis in mollusks is not well understood yet. Until now, several genes related to regulate and product melanin have been cloned and analyzed, such as *Pax3/7* from *Pinctada fucata*, *Mizuhopecten yessoensis* and *Aplysia californica* (Navet et al., 2017), *Mitf* from *Meretrix petechialis* (Zhang et al., 2018), *Tyr* from *P. fucata* (Takgi and Miyashita, 2014), *M. meretrix* (Yao et al., 2020) and *C. gigas* (Zhu et al., 2021). Despite extensive investigations have mined omics data to identify genes of pigmentation pathway in bivalves, the melanin synthesis pathway is still largely speculative and no clear axis or pathway predicted in bivalves so far (Saenko and Schilthuis, 2021).

The *Pax* genes encode evolutionarily conserved transcription factors that play critical roles in development. Among these, *Pax3/7* gene acts on nervous system development, skeletal muscles and chromocyte

Abbreviations: arf1, adp-ribosylation factor 1; CRE, cAMP response element; Cdk2, cyclin-dependent kinase; e1 α , α subunit of elongation factor 1; EGFP, enhanced green fluorescent protein; Gapdh, glyceraldehyde-3-phosphate dehydrogenase; HD, homeobox domain; Mitf, microphthalmia-associated transcription factor; Pax, Paired-box; PRD, paired domain; RNAi, RNA interference; TEM, transmission electron microscopy; TYR, tyrosinase; TYRP1, tyrosinase-related protein 1; TYRP2/DCT, tyrosinase-related protein 2; WMISH, whole mount in situ hybridization.

* Correspondence author at: Key Laboratory of Mariculture, Ministry of Education, Ocean University of China, Qingdao, China.

E-mail address: qili66@ouc.edu.cn (Q. Li).

<https://doi.org/10.1016/j.cbpb.2022.110720>

Received 13 October 2021; Received in revised form 8 February 2022; Accepted 11 February 2022

Available online 14 February 2022

1096-4959/© 2022 Elsevier Inc. All rights reserved.

formation (Lang et al., 2007; Nord et al., 2016). *Pax3/7* subfamily is an ortholog of vertebrates *Pax3* and *Pax7* genes, which have structural and functional similarities (Hayashi et al., 2010; Blake and Ziman, 2014). In mollusks, *Pax 3/7* gene has been identified and characterized by the presence of a PRD, HD and octapeptide. Until now, the octapeptide was only obvious in cephalopods and several bivalves (Navet et al., 2017). Studies on gene expression are available where the *Pax3* is frequently expressed in nervous system of cephalopods (Scherholz et al., 2017). Moreover, *Pax3/7* is also capable of regulating melanin synthesis and has potential strategy to increase the efficacy of anti-melanogenesis (Lang et al., 2005; Lee et al., 2018; Medic and Ziman, 2010). To our knowledge, only one recent article reported that *Pax3* gene functioned in controlling melanin synthesis in *Pteria penguin* (Yu et al., 2018b), but no extensive search has addressed the role in melanin synthesis of *Pax3/7* in other bivalves.

The Pacific oyster (*C. gigas*) is a bivalve mollusk of high interest in biological research and as an economic resource. In present study, *Pax7* gene from *C. gigas* was characterized and its expression was analyzed. The *Pax7* gene function was deliberated by RNAi technology, which has been applied in bivalves, such as *C. gigas* (Choi et al., 2013; Fabioux et al., 2009; Huvet et al., 2012, 2015), and *P. penguin* (Yu et al., 2018b). Silencing target gene by feeding dsRNA-expressing bacteria, is an inexpensive and high output technique to produce large quantities of dsRNA (Ipsaro and Joshua-Tor, 2015). After knocking down the expression of *Pax7*, the transcriptional level of genes related to melanin synthesis decreased by qPCR detection. In addition, tyrosinase activity was declined and melanin granules were less and defected by light and electron microscopes observation. This study proposed the function of *Pax7* in melanin synthesis of *C. gigas*.

2. Materials and methods

2.1. Sample collection

Sexually mature adults of Pacific oysters with whole black shell were obtained from Rongcheng, Shandong province, China. The oysters were cultivated with the recirculating seawater at 23–25 °C for 7 days in laboratory before sampling. Aeration was provided and oysters were fed with *Chlorella vulgaris* three times daily (08:00, 14:00 and 20:00). To mimic the practical water exchange, the 60% of water volume was renewed with aerated water (24 ± 1 °C) before 08:00 and 20:00. After adaptation, the oysters (shell length 48 ± 5.88 cm, shell height 82.15 ± 8.26 cm) were randomly chosen for next experiment. Six tissues, including mantle edge, central mantle, gill, labial palp, adductor muscle and digestive gland were sampled for RNA isolation. For embryonic and larval sampling, oysters with black shell color were transferred to Litao hatchery, Laizhou, Yantai, Shandong province, and conditioned at ambient conditions (temperature 24 ± 1 °C, salinity 30.5 ± 0.5 psu) prior to experiment. Adult oysters with 30 males and 30 females (shell length 93.54 ± 1.81 cm, shell height 56.94 ± 1.83 cm) were dissected. Sperm and oocytes collected were mixed and incubated in 20 L bucket about 1 h with gentle shaking. Fertilized eggs were reared at a concentration of 50 eggs/ml under optimal condition (temperature 23–25 °C, salinity 30–31 psu). Larvae were fed daily with a mixture of *Isochrysis galbana* and *Chaetoceros calcitrans* at concentrations ranging from 30,000 to 80,000 cells/ml, depending on age. Development of the embryos and larvae were observed under the microscope. Embryos and larvae at different developmental stages, including fertilized egg, blastula, gastrula, trochophore, D-shaped larvae 1/2, umbo larva 1/2 and eyed-larva, were collected (Table 1). Same-staged larvae (over 80% larvae belong to the same stage larvae) were placed in RNA storage reagent and stored at –80 °C until use for RNA extractions. For WMISH, samples before D-shaped larvae were pre-fixed overnight at 4 °C in 4% PFA. Samples from D-shaped larvae to eyed-larvae were firstly relaxed by gradually adding 7.5% magnesium chloride aqueous solution until the valves gaped open and the vela were fully extended. After relaxation,

Table 1

Larval developmental stages of *C. gigas*.

Developmental stages	Sampling time (after fertilization)
Fertilized egg	1 h
Blastula	5 h
Gastrula	8 h
Trochophore	11 h
D-shaped larvae 1	24 h
D-shaped larvae 2	2 days
Umbo larva 1	10 days
Umbo larva 2	16 days
Eyed-larva	28 days

larvae were fixed in 4% PFA. Then all samples transferred into methanol and stored at –20 °C.

2.2. Sequence analysis of *CgPax7*

The amino acid sequences of *Pax7* in *C. gigas* (*CgPax7*, XP_011424860.2) and *Pax3/7* from other organisms, including *C. virginica* (*CvPax7-like*, XP_022344121.1), *Pteria penguin* (Röding, 1798) (*PpPax3*, MH558581), *Mizuhopecten yessoensis* (*MyPax3*, XP_021364914.1), *Mytilus edulis* (*MePax3/7*, CAG2237822.1), *Mytilus galloprovincialis* (*MgPax3/7*, VDI32574.1), *Branchiostoma belcheri* (*BbPax3/7*, ABK54280.1), *Danio rerio* (*DrPax7a*, NP_571400.1), *Xenopus laevis* (*XlPax7*, XP_018080096.1), *Gallus gallus* (*GgPax7*, NP_990396.1), *Mus musculus* (*MmPax7*, NP_035169.1), *Homo sapiens* (*HsPax7*, NP_001128726.1), were retrieved from NCBI database. The gene function domain of amino acid was predicted using the SMART database (<http://smart.embl-heidelberg.de/>). The sequences were aligned using Clustal X 2. Based on the alignment, phylogenetic tree was constructed by the maximum-likelihood algorithm with JTT + G + I model using the MEGA X software.

2.3. Gene expression analysis by real-time quantitative PCR

Total RNA was isolated using Trizol Reagent (Invitrogen, CA, USA) according to the manufacturer's instructions. Each RNA sample integrity was examined on 1.2% agarose gel and the concentration and purity was checked with Nanodrop 2000 (Thermo scientific, USA). First strand cDNA was synthesized using PrimeScript™ RT reagent Kit with gDNA Eraser (Takara, China) following the manufacturer's protocol. In brief, 1 µg total RNA of each sample was used in 20 µL reaction and the concentration of cDNA products is 200 ng/µL. First, the gDNA Eraser was used to remove genomic DNA. Subsequently, the synthesis of cDNA was performed using PrimeScriptRT Enzyme Mix I and RT Primer Mix contained Random 6 mers and Oligo dT Primer. The qPCR primer pairs (listed in Table 2) for target genes and three reference genes, such as *ef1α*, *arf1* and *gapdh* (Du et al., 2013; Huan et al., 2016), were designed with Primer 3 from NCBI (<https://www.ncbi.nlm.nih.gov/tools/primer-blast/>). *Ef1α*, *arf1* and *gapdh* genes were used as internal control. QuantiNova™ SYBR® Green PCR Kit following the instruction manual of the kit (QIAGEN, Germany) on LightCycler 480 real-time PCR instrument (Roche Diagnostics, Burgess Hill, Switzerland). The 10 µL qRT-PCR reaction contained 5 µL 2× SYBR Green PCR Master Mix, 1 µL of each primer (10 µM) and 1 µL cDNA (200 ng/µL). The thermal cycling profile consisted of an initial denaturation at 95 °C for 2 min, 40 cycles of denaturation at 95 °C for 5 s, annealing at 60 °C for 10 s, followed by melt curve analysis (65–95 °C) to confirm the qPCR specificity. All qPCR reactions were performed in triplicate for each cDNA sample. Before experiment, all genes were detected by standard curve to confirm the specificity of primers. The relative expression levels of target genes were normalized with the reference gene. Gene expression was measured using 2^{–ΔΔCT} method (Livak and Schmittgen, 2001) and subsequently expressed in fold-differences. All data were shown as mean ± standard error (n = 6).

Table 2
Sequences information of Specific Primers.

Gene name	Primer	Sequence (5'-3')	Application
Pax7, Paired-box 7	<i>CgPax7</i> -F	AATGCCTCAGAGACGGAAA	WISH/qPCR
	<i>CgPax7</i> -R	GGAAGGGTCTGCCGTTAAT	WISH/qPCR
	<i>CgPax7-Not1</i> -F	AAATATGCGGCCGCTCATCGGAGGAAGCAAACCC	RNAi
	<i>CgPax7-Hind</i> -R	CCAAGCTT TTCCGCCGTGAAAGTAGTCC	RNAi
	<i>CgPax7-Not</i> 1-F	ATAAGAATGCGGCCGCTCTGAAGACGAAGAGCCCA	RNAi
	<i>CgPax7-Hind</i> -R	CCAAGCTTAGAGGGTAACTGGGAGTGGT	RNAi
	<i>CgPax7-1-I</i> -F	TCATCGGAGGAAGCAAACCC	RNAi
	<i>CgPax7-1-I</i> -R	GGACGGACGATCTGTACAAA	RNAi
	<i>CgPax7-1-O</i> -F	GAGGCTCGAGTCCAAGTCTG	RNAi
	<i>CgPax7-1-O</i> -R	AAGGTATGAAGAAGCGCCCC	RNAi
	<i>CgPax7-2-I</i> -F	ACGGCCTTGTGCATAAGCA	RNAi
	<i>CgPax7-2-I</i> -R	GGGACGGATGCTTCCTGTTT	RNAi
	<i>CgPax7-2-O</i> -F	GTGACGTCATCAGTATCCGCT	RNAi
	<i>CgPax7-2-O</i> -R	CGAGACTTCATTGCAACGC	RNAi
	EGFP, enhanced green fluorescent protein	EGFP-F	AGCTTAGCAAGGGCGAGGAGCTG
EGFP-R		GCGCTTACTTTGTACAGCTCGTCCATGCC	RNAi
TYR, tyrosinase	Tyr-F	GTACGATTCCTGTGGTCCGGC	qPCR
	Tyr-R	GAGGTGAAGCGTCATCCAAAG	qPCR
TYRP1, tyrosinase-related protein 1	Tyrp1-F	CGAGGCGTTTCCAGTTTGTG	qPCR
	Tyrp1-R	TGGCAGTAGCCGGTGAATTT	qPCR
TYRP2, tyrosinase-related protein 2	Tyrp2-F	TCGTCGATGAAAGGCAACCA	qPCR
	Tyrp2-R	CATACACTGGACAAGCGGGT	qPCR
Mitf, microphthalmia-associated transcription factor	Mitf-F	CAGAGGGAGACGAACAGACG	qPCR
	Mitf-R	ATATCGATACCCCGTCCGA	qPCR
Cdk2, cyclin-dependent kinase	Cdk2-F	AGGTGTGCCAAGTACAGCAA	qPCR
	Cdk2-R	ACACCAAGTACAGCTTCTGCT	qPCR
Efl α , α subunit of elongation factor 1	Efl α -F	ACGAATCTCTCCAGAGGCT	qPCR
	Efl α -R	GAAGTTCTTGGCCGCTTTG	qPCR
Arf1, adp-ribosylation factor 1	Arf1-F	TCAGGACAAGATCCGACCACTGT	qPCR
	Arf1-R	GCAGCGTCTCTAAGTTCATCCTCATT	qPCR
Gapdh, glyceraldehyde-3-phosphate dehydrogenase	Gapdh-F	AGAACATCGTCAGCAACGCATCC	qPCR
	Gapdh-R	CCTCTACCACCAAGCCAATCTC	qPCR

2.4. Whole mount *in situ* hybridization

The gene specific primers for probe synthesis are shown in Table 2. The linear template for probe synthesis was generated via PCR using 2× Taq Plus Master Mix (Vazyme, Nanjing, China). Amplified products were purified using GeneJET PCR Purification Kit (Thermo Fisher Scientific, Waltham, MA, USA) and subsequently used as templates for sense and anti-sense RNA probe syntheses. Synthesis reaction was performed using a DIG RNA Labeling Kit (T7) (Roche Life Science), following the manufacturers' instructions. WMISH was conducted as described previously with some modifications (Yang et al., 2012). In brief, fixed larvae were rehydrated through methanol into 0.1% Tween-20 in PBS (PBST). Samples from D-shaped larvae to eyed-larvae were decalcified in 0.5 M EDTA for 30 min-7 h, subsequently, all samples were digested with 1 μ g/mL proteinase K at 37 °C for 30 min. Prior to the hybridization, treated larvae were incubated in hybridization buffer at 65 °C for 5 h. Then larvae were hybridized with 200 ng/mL sense and antisense probe at 65 °C overnight, respectively. After unbound probes were washed away, antibody incubation was performed with 1/5000 anti-digoxigenin antibody (Roche) in blocking reagents at 4 °C overnight. Samples were then washed several times in MABT, and in alkaline tris buffer for 10 min twice. Color development were performed with 2% NBT/BCIP solution in darkness at room temperature for 2 h. After washing, images were photographed on a fluorescent microscope (Olympus BX53) with a digital camera (Olympus DP73). The method of allocation reagents used in WISH was listed in Table S1.

2.5. RNA interference experiment

DNA fragments of *CgPax7-1* and *CgPax7-2* were amplified by PCR using specific primers (Table 2). EGFP was used as a negative control (NC) in experiment. Vector construction and expression of dsRNA experiment were performed following sub-cloning, ligation, transfection and induced expression, the same methods previously described in

detail by reference (Feng et al., 2019; Hu et al., 2021). RNA extraction was performed on non-induced *E. coli* and IPTG-induced *E. coli* transformed with a specific gene using Bacteria RNA Extraction Kit (Vazyme, Nanjing, China).

In RNAi experiment, three dsRNA-producing bacteria were prepared by inducing *E. coli* strain HT115 (DE3) bacteria transformed with three constructed plasmids (*CgPax7-1*-L4440, *CgPax7-2*-L4440 and EGFP-L4440) with isopropyl β -D-thiogalactoside (IPTG), respectively. Algae/bacteria co-inoculum was produced by mixing algal culture and bacterial suspension at a ratio of 100 bacteria per algal cell, with a final *p. subcordiformis* concentration of 25,000 cells/mL and *Nitzschia closterium f. minutissima* concentration of 35,000 cells/mL. The ratio was optimized by increasing algal concentration according to Payton et al. (2017). During the experiment, food reserves were renewed with fresh algae/bacteria co-inoculum every 24 h. Specifically, *E. coli* strain HT115 bacteria containing recombinant plasmid were grown at 37 °C overnight with shaking in LB with ampicillin (50 μ g/mL) and tetracycline (12.5 μ g/mL). Five milliliters of overnight bacteria were cultured in 500 mL of fresh LB medium containing resistance and until OD₅₉₅ upped to 0.4. dsRNA production was induced by 0.4 mM IPTG at 37 °C for 4 h. Then, induced bacterial cultures were centrifuged and bacterial pellets were resuspended in 500 mL *Platymonas subcordiformis* and 125 mL *N. closterium f. minutissima* algae culture liquid. Bacteria adsorption rate on the algae was evaluated by preliminary experiments (Feng et al., 2019). The adsorption rate was assessed as the ratio between the number of colonies from filtrated suspension and from total inoculum, which was calculated as 99%. Concentrations of algae and bacteria were monitored daily with 2800 UV-visible spectrophotometer (Unico, USA) for the duration of the experiment.

During the interference phase of larvae, Umbo larvae (180 μ m) with black shell in three buckets (400 L) were fed with Alga/dsRNA-producing bacteria co-inoculum at 8:00 and fed with *P. subcordiformis* and *N. closterium f. minutissima* at 14:00 and 20:00. The density of larvae was 2 larvae/ml in each bucket. The sea water was maintained at

23–25 °C and fresh air was continuously pumped into each bucket. To mimic the practical water exchange, the 60% of water volume was renewed with aerated water (24 ± 1 °C) before 08:00 and 20:00. There are a few deaths in three buckets but no significantly differences in three buckets, and it also happened in normal breeding pond. After 15 days, larvae collected for RNA extraction. For RNAi experiment in adult oysters, one-year-old oysters with the whole black shell were cultivated with the recirculating seawater at 23–25 °C for 10 days before the experiment. The oysters (shell length 48 ± 5.88 cm, shell height 82.15 ± 8.26 cm) were selected to perform RNAi experiment for a month. The details about RNAi feeding procedures were as following in references (Feng et al., 2019; Hu et al., 2021). Briefly, ten oysters in *CgPax7*-2-RNAi group and EGFP-RNAi group were carried out in adult oysters, respectively. Adult oysters were also fed with Alga/dsRNA-producing bacteria co-inoculum at 8:00 and fed with *P. subcordiformis* and *N. closterium f. minutissima* at 14:00 and 20:00. The 60% of water volume was renewed with aerated water (24 ± 1 °C) before 08:00 and 20:00. After 30 days, no oyster died during exposure experiments and mantles were collected for the following RNA extraction, gene expression, tyrosinase activity assay and microscopy examination. In terms of gene expression, the detection of RNAi products (interest gene dsRNA) was assessed as the mean ± SE of individuals $2^{-\Delta\Delta Ct(Cg_{inside})-\Delta\Delta Ct(Cg_{outside})}$, i.e., the ratio of the *CgPax7* mRNA level measured with primer sets *CgPax7*-I (quantification of both endogenously expressed *CgPax7* mRNAs and *CgPax7* dsRNAs) to the *CgPax7* mRNA level obtained with primer sets *CgPax7*-O (to quantify the endogenously expressed *CgPax7* mRNAs). Therefore, this ratio is equal to (gene dsRNAs + gene mRNAs)/gene mRNAs = (gene dsRNAs/gene mRNAs) + 1.

2.6. Tyrosinase activity assay

Tyrosinase activity assays were performed in mantle of adult oyster in *CgPax7*-RNAi group and EGFP-RNAi group using tissue tyrosinase activity assay kit (Solarbio, Beijing, China, Art. No. BC4050). Briefly, 0.1 g mantle tissue was homogenized in 1 ml phosphate buffer solution and was centrifuged at 12,000 g for 20 min to obtain the supernatant. Then, 0.1 ml of tissue supernatant and 0.9 ml buffer containing L-dopamine were mixed together and incubated at 25 °C for 50 min. The absorbance at 475 nm (UV-2800A, Unico, Shanghai) of mixture was measured at 10 s and 50 min. One unit of tyrosinase activity was defined as the amount of activity that produced 1 nmol of dopachrome per minute via the hydroxylation of tyrosine by the standard tyrosinase at 25 °C and expressed as nmol/g wet weight.

2.7. Microscopy

Mantle tissues from adult oysters were collected after RNAi experiment and processed for various microscopic characterizations to assess histological structure changes of mantle (especially melanosomes and melanin granules) using the same methods and equipment previously described by Ruska et al. (2020). Briefly, for histology samples, mantle was fixed directly with Bouin' solution, dehydrated in ethanol, cleared with xylol, embedded in paraffin wax and sectioned (5 µm). Afterward, the slides were deparaffinized and stained with hematoxylin and eosin (H&E) dye in preparation for histological examinations under an Olympus BX53 light microscope. For TEM, tissue processing for the ultrastructure analysis was performed according to Wang et al. (2020). Briefly, the isolated mantle with 1 mm³ was fixed in 2.5% glutaraldehyde at 4 °C. Specimens were washed in 0.1 M phosphate buffer (pH 7.0) for 15 min, dehydrated in ethyl alcohol in 1% osmium tetroxide for 1 h before post-fixation, then immersed in propylene oxide and embedded in LR White resin. Ultrathin sections (60–80 nm) obtained were stained with uranyl acetate, then with lead citrate (Reynolds, 1963), and examined under a JME-1200EX transmission electron microscope (JEOL, Japan) operated at 80 kv.

2.8. Statistical analysis

The significance of difference analysis was performed using SPSS 17.0, *t*-test and one-way analysis of variance (ANOVA) method was used to detect between two data and multiple data, respectively. *P* < 0.05 was considered statistically significant.

3. Results

3.1. Sequence analysis of *CgPax7*

In the deduced 463-aa *CgPax7* protein, a Pax domain (site 41–165), a Hox domain (site 230–292) and octapeptide were identified (Fig. 1A). Amino acid sequence alignments of *Pax7* gene from *C. gigas* and other species were performed. The *CgPax7* shared the highest (84.67%) identify with *Pax7* of *C. virginica*, 64.32% with *M. edulis*, 63.83% with *M. galloprovincialis*, 64.67% with *Pax3* of *P. penguin*, 60.38% with *Pax3* of *M. yessoensis*. The deduced amino acid sequence comparison revealed a highly conserved N-terminal PRD containing 127 amino acids, octapeptide motif and a HD containing 59 amino acids (Fig. 1B).

Phylogenetic analysis was performed with the ML method based on multiple sequence alignment of *C. gigas* as well as other mollusks and animal counterparts. As expected, *CgPax7* was closest to *Pax7* of *C. virginica* and *Pax3* of *P. penguin*, with a support of 78%. Three *Pax3* or *Pax3/7* genes of bivalves referred, including *M. yessoensis*, *M. edulis* and *M. galloprovincialis* were grouped into a close cluster. All *Pax7* or *Pax3/7* genes of vertebrates referred were classified to a big clade, which exhibited farther distance to *Pax7* of invertebrates (Fig. 1C).

3.2. Temporal and spatial expression of *CgPax7* gene

Transcription level of *CgPax7* was analyzed by qPCR in embryolarval stages (Table 1) and various tissues. The primer specificity of *Pax7* is listed in Table S2. *CgPax7* were expressed robustly in all embryolarval stages, with expression in D-shaped 2 stage significantly higher than that in other stages (Fig. 2A). In adult oyster, the mRNA transcripts of *Pax7* were detectable in a range of tissues, in the following order of expression (high to low): adductor muscle > central mantle > gill > mantle edge > labial lap > digestive gland (Fig. 2B). Next, the spatial pattern of *CgPax7* mRNA expression was mapped by WMISH from fertilized eggs to eyed-larvae (Fig. 3). WMISH analysis showed that *CgPax7* exhibited obviously distinct spatial patterns, which was generally consistent with the real-time PCR results. No strong *CgPax7* mRNA signals were detected in embryos of egg, blastula, gastrula and trochophore larvae. The *CgPax7* signal was detected at D-shaped stage 1, it was stronger on margins of the growing valves and hinge region (Fig. 3E-F). At D-shaped stage 2, a higher level of *CgPax7* transcript was limited to margins of the growing valves, but signal was barely visible in the hinge region (Fig. 3G). At umbo larvae stages, gene expression was also concentrated in margins of the shell valves (Fig. 3I-K). At eyed-larva stage, The *CgPax7* mRNA signals began to decrease and became undetectable (Fig. 3L). No signal was found in control experiments performed in parallel on the same batch of embryo-larval with the corresponding sense RNA riboprobe (Fig. S1).

3.3. *CgPax7* expression was inhibited by RNA interference in *C. gigas*

RNAi was performed to investigate the function of *CgPax7* gene. The primer specificity of genes is listed in Table S2. Initially, the expression results of dsRNA induced in *E. coli* shown that bands of dsRNA corresponding to the *Pax7*-1, *Pax7*-2 gene plus sequence between two T7 promoters of about 200 bp was observed in the IPTG-induced *E. coli* transformed with *Pax7*-1 and *Pax7*-2 construct (Fig. S2 B), but not in the noninduced *E. coli* transformed with *Pax7*-1 and *Pax7*-2 construct (Fig. S2 B), indicating the successful expression of dsRNA in *E. coli*. Then, to evaluate the effects of dsRNA delivery by feeding, the qPCR was

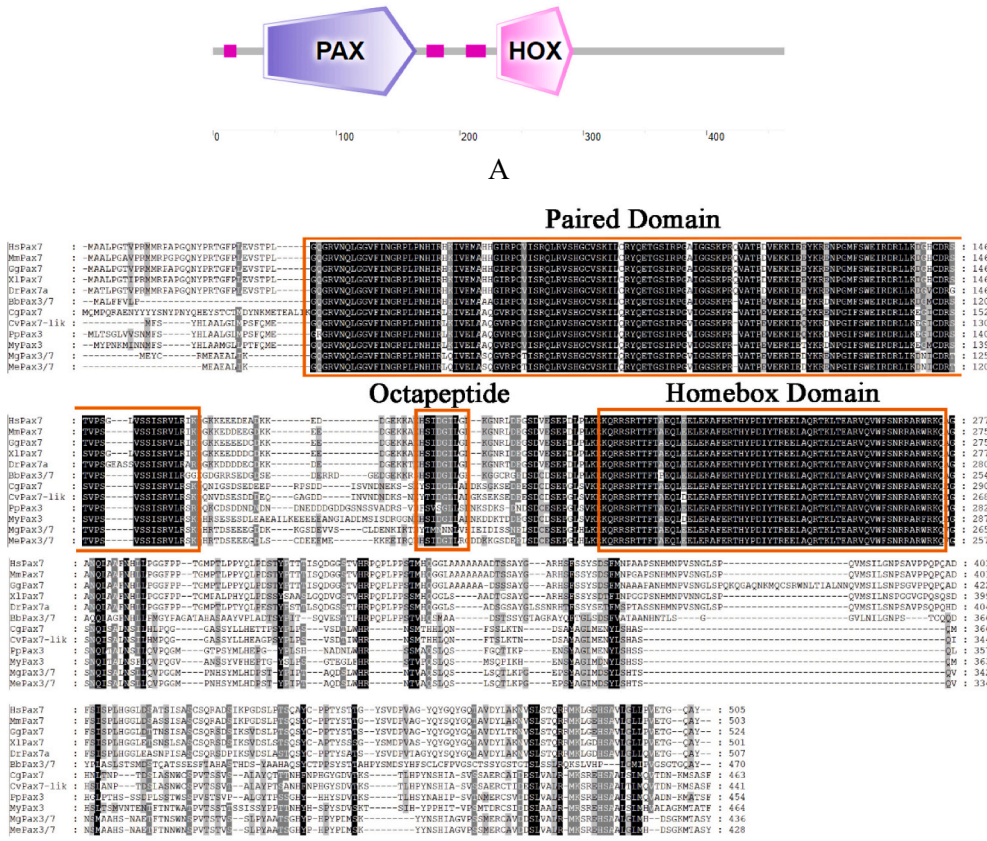


Fig. 1. Sequence alignment and phylogenetic analysis. (A) A scheme of *CgPax7* gene. Pax domain and Hox domain were predicted. (B) Comparison of deduced amino acid sequence of *Pax7* or *pax3/7* among different species. The predicted conserved features were in orange box. (C) Phylogenetic tree based on the amino acid sequences of *Pax3/7*. The numbers at the nodes indicated the percentage frequencies in 1000 bootstrap replications. GenBank accession numbers of the sequences followed the name of the species. ♦ meant the *Pax7* of *C. gigas*.

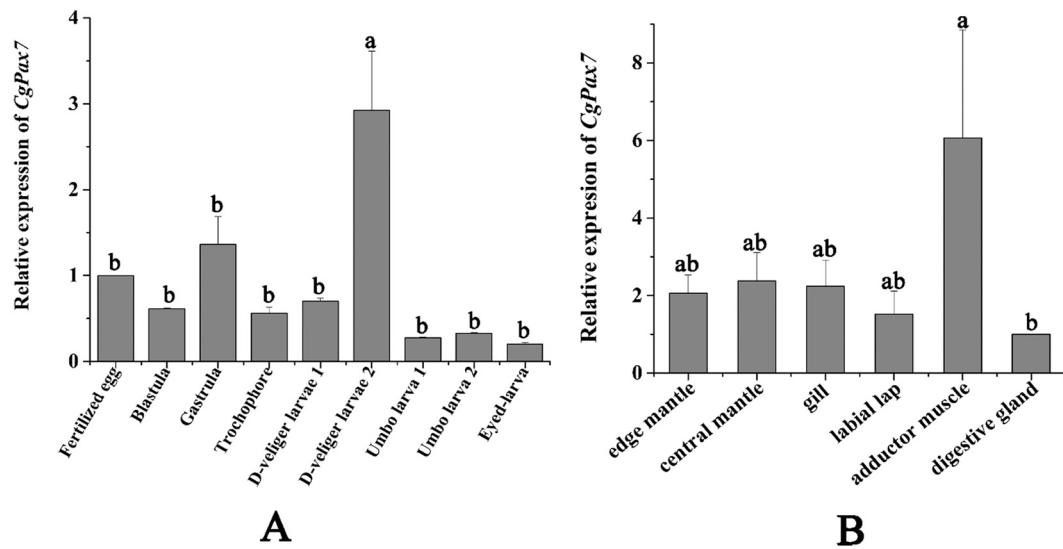


Fig. 2. Expression analysis of *CgPax7* gene estimated by qPCR. The different letters above the error bars indicated significant differences ($P < 0.05$). All data were shown as mean \pm standard error (SE) ($n = 6$). (A) Expression profiles of *CgPax7* during embryonic and larval development. The full name of different developmental stages was shown in Table 1. The fertilized egg was used as control. (B) Expression patterns of *CgPax7* in different tissues. The digestive gland was used as control.

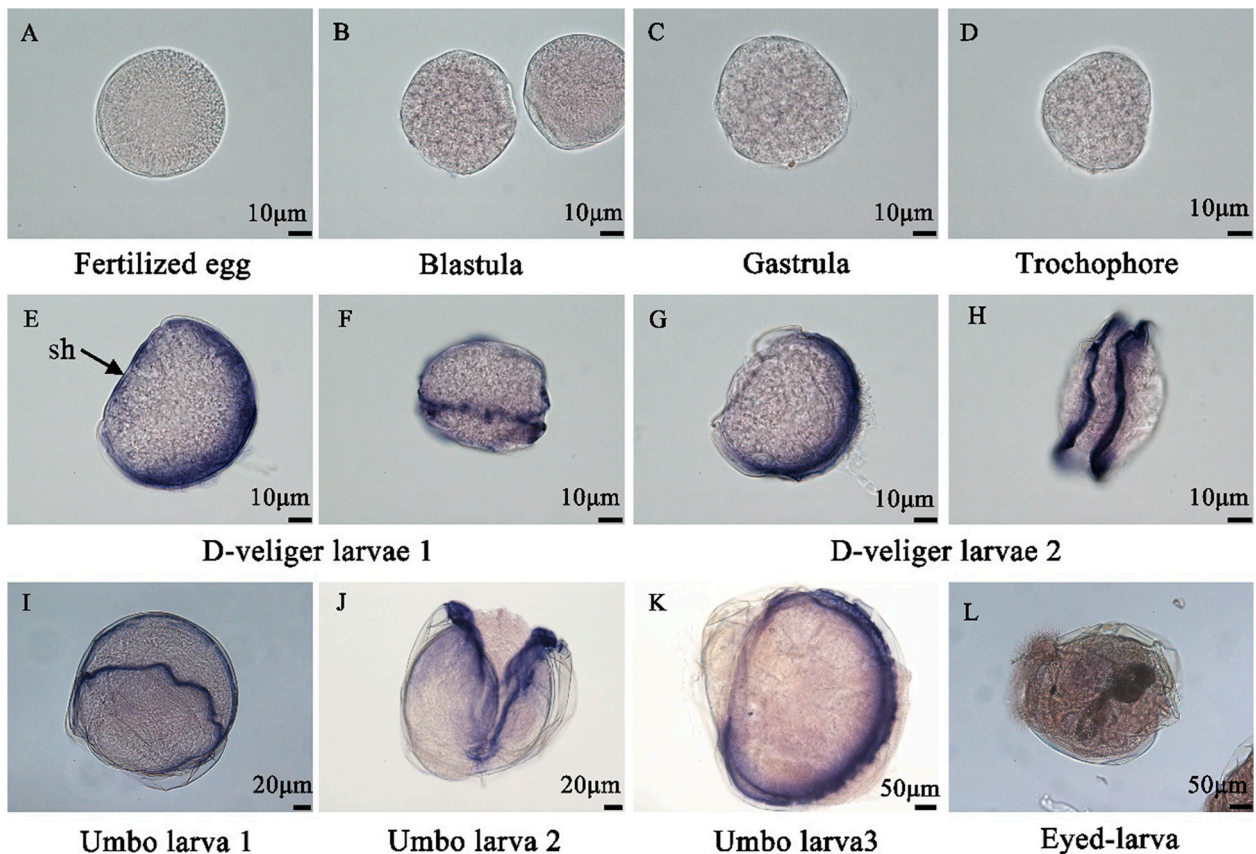


Fig. 3. The spatial pattern of *CgPax7* mRNA localization during embryonic and larval development. The black arrows indicated the shell hinges (sh). Note the intense signal in the growing valves in D-shaped stage 2 and umbo larvae (G, I–K). Bars in A–H are 10 μ m, bars in I and J are 20 μ m, bars in K and L are 50 μ m.

employed to detect EGFP dsRNA in oysters fed on bacteria containing the EGFP-L4440 plasmid. The detection of RNAi product was assessed as a function of the ratio of the interfering *CgPax7-1/CgPax7-2* dsRNA to endogenous *CgPax7-1/CgPax7-2* mRNA level. The levels of dsRNAs were 1.1 and 1.9 times more abundant than endogenously expressed

mRNAs in *CgPax7-1/CgPax7-2* dsRNA in larva, respectively (Fig. S3A). The ratio was 9.3 in mantle of adult oyster (Fig. S3B).

The efficiency of interference was determined by qPCR, *CgPax7* expression was detected after 15 days in larvae and 30 days in adult oyster, respectively. In this study, EGFP dsRNA group was used as

negative control (NC). In RNAi of larva, compared with NC group, expressions of *CgPax7-1* and *CgPax7-2* were reduced by 13.8% in *CgPax7-1* group and 73.6% in *CgPax7-2* group ($P < 0.05$), respectively (Fig. 4A). There was no doubt that *CgPax7-2* dsRNA feeding was effective in knocking down the expression of *CgPax7*. Hence, In RNAi of adult oyster, only *CgPax7-2* dsRNA feeding experiment was performed and qPCR results displayed the *CgPax7-2* expression was significantly reduced by 60.1% ($P < 0.05$) compared to the NC group (Fig. 4B).

3.4. Effect of *CgPax7* silencing on the expression of *CgMitf*, *CgTyr*, *CgTyrp1*, *CgTyrp2* and *CgCdk2*

As the potential downstream gene of *CgPax7* and melanin synthesis related genes, *CgMitf*, *CgTyr*, *CgTyrp1*, *CgTyrp2* and *CgCdk2* genes were detected for its mRNA expression change in *CgPax7*-suppressed individuals by qPCR. As shown in Fig. 4C and D, *CgTyr* is a key rate-limiting enzyme in melanin synthesis and its expression was significantly down-regulated by 94.59% ($P < 0.05$) in larvae, interestingly, it was highly raised in mantle of adult oysters. *Tyrp1* and *Tyrp2* was related to the melanocyte differentiation and migration, after *CgPax7* silencing, *CgTyrp1* and *CgTyrp2* gene expression was highly decrease by 82.24% ($P < 0.05$) and 89.66% ($P < 0.05$) in larvae as well as 72.19% ($P < 0.05$) and 55.71% ($P < 0.05$) in mantle of adults, respectively. The

CgCdk2, a melanocyte growth-dependent kinase, its transcript level was also depressed by 58.32% ($P < 0.05$) and 34.68% ($P < 0.05$) in larvae and mantle of oysters, respectively. Nevertheless, as a center transcription factor of melanogenesis, *CgMitf*, its expression was no significant difference after *CgPax7* knockdown.

3.5. *CgPax7* silencing depressed tyrosinase activity

The tyrosinase activity in mantle of adult oysters after *CgPax7* silencing was shown in Fig. 5. The tyrosinase activity was obviously decreased about 65.87% in *CgPax7*-RNAi group compared with NC group ($P < 0.05$), which was generally consistent with the gene expression result (Fig. 4D). This indicated that *CgPax7* obviously affect the tyrosinase activity in *C. gigas*.

3.6. Morphology changes of mantle after *CgPax7* silencing

Visual inspection showed that the color of mantle edge is different between two groups, *CgPax7-2* group exhibited obvious shallow than that in control group (Fig. 6A). The effects of *CgPax7-2* silencing on histological sections of mantle edge were illustrated in Fig. 6B. Similarly, the epithelial tissue of mantle edge in *CgPax7-2* group displayed less brown-granules than that in control group, indicating that *CgPax7*

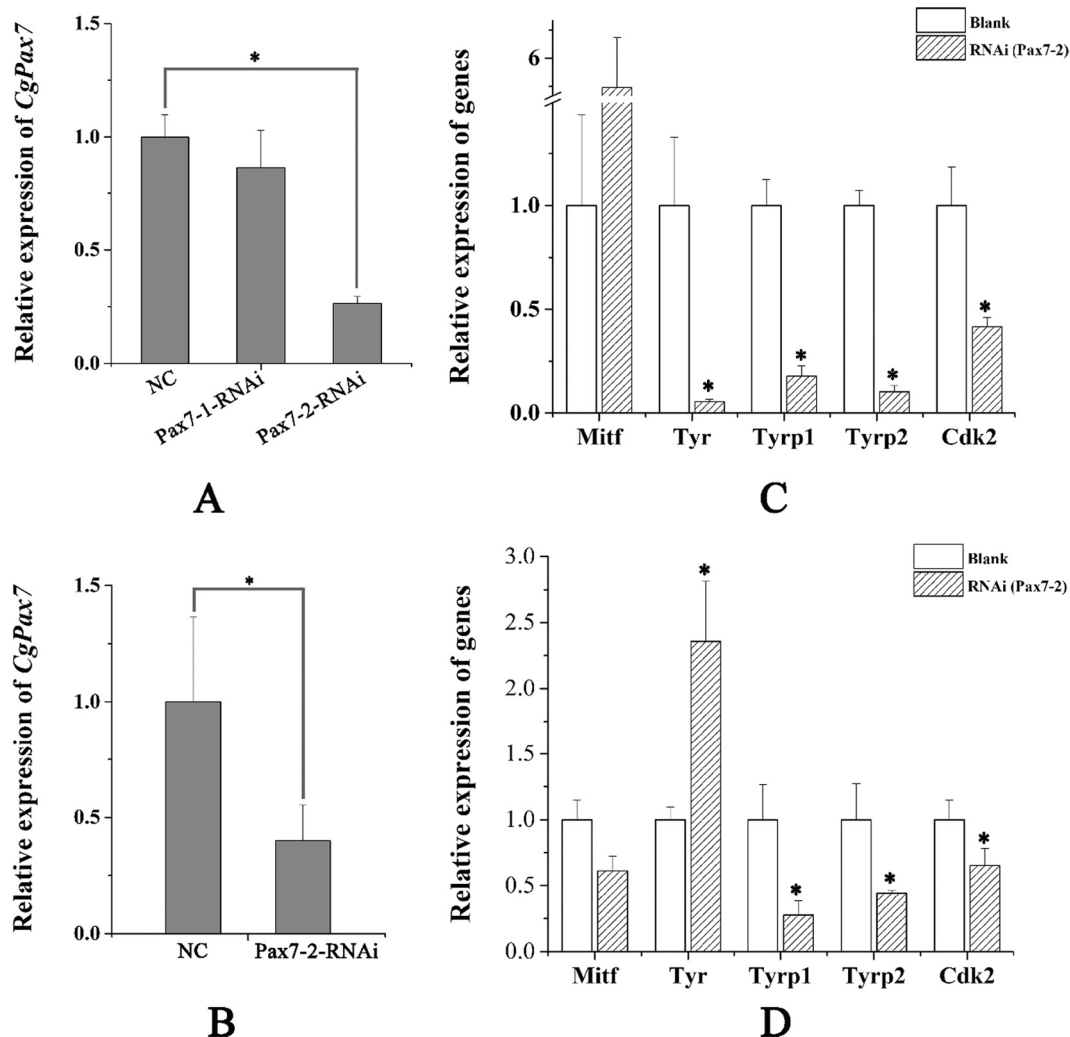


Fig. 4. Expressions of *CgPax7*, *CgMitf*, *CgTyr*, *CgTyrp1*, *CgTyrp2* and *CgCdk2* after *CgPax7* silencing. (A, B) Expressions of *CgPax7* in larvae and mantle, respectively. (C, D) Expressions of *CgMitf*, *CgTyr*, *CgTyrp1*, *CgTyrp2* and *CgCdk2* in larva as well as mantle, respectively. The qPCR was done with RNA samples from EGFP-RNAi group (NC) and *CgPax7-2* silencing group (*CgPax7-2*-RNAi). The *efl α* of *C. gigas* was used as an internal control. All data were shown as mean \pm SE ($n = 6$). Significant difference was indicated by * ($P < 0.05$).

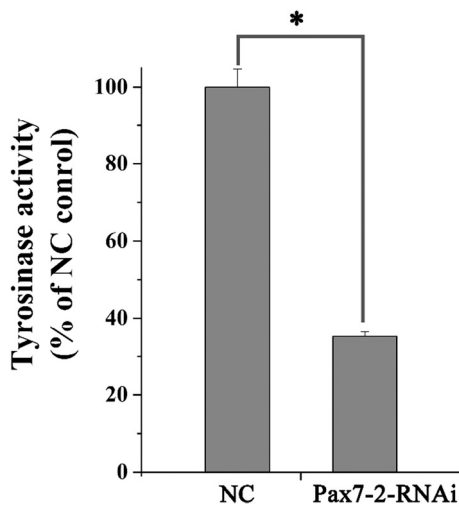


Fig. 5. Tyrosinase activity in control and *CgPax7* silencing groups. The tyrosinase activity was performed with samples from EGFP-RNAi group (NC) and *CgPax7-2* silencing group (Pax7-2-RNAi). The tyrosinase activity was shown with percentage of every group and NC. All data were shown as mean \pm SE ($n = 6$). Significant difference was indicated by * ($P < 0.05$).

silencing blocked the melanin synthesis. To getting more insights into cellular basis of melanin granules in mantle, TEM of oyster mantle was performed (Fig. 6C). In control group, uniformly dense and evenly distributed melanosome of round-to-oval or round shape and smooth edge were present in epithelial tissue (Fig. 6C a1-a2) and connective tissue (Fig. 6C a3-a4) in mantle edge. In Pax7-2 knockdown individuals, melanosomes were smaller and less densely pigmented than that in the control (Fig. 6C b1-b4). For some melanosomes, membrane integrity was completely disrupted resulting in rough edge. This was the case in melanosome of connective tissues (Fig. 6C b3-b4, Fig. S4). Therefore, the mantle color of Pax7-2 silencing oyster was obviously connected to melanosomes defects.

4. Discussion

The shell coloration is the most tractable indicator for evaluating its quality and value in mollusks. It has long been assumed that melanin is the main contributor to pigmentation of shell. Melanocytes are responsible for synthesis and storing melanin, melanin synthesis are regulated by many common genes. Recently, the link between Pax3/7 gene and melanophore was interested in many researches (Blake and Ziman, 2014; Fang et al., 2022; Roberts et al., 2016). In this study, we revealed for the first time, the molecular characterization and function on pigmentation of Pax7 gene from *C. gigas*.

4.1. Molecular characterization of Pax7 gene in *C. gigas*

The putative amino acid sequence of *CgPax7* is similar with other Pax7 or Pax3/7, displaying the highest identify (Fig. 1B). The two domains, PRD and HD, recognized by specific DNA sequences (Lang et al., 2007) were conserved in aligned vertebrates and invertebrates. An additional conserved domain found in most amino acid sequences, is octapeptide motif (H(Y)SIDGILG(A)), functions as a transcriptional inhibitory motif (Lang et al., 2007). This motif was existed in bivalves, including *C. gigas*, *C. virginica*, *M. yessoensis* and *M. edulis*, which was further refined the previous report (Scherholz et al., 2017). Pax7 gene is a member of Pax3/7 subfamily in vertebrates, with a purpose to explore the orthologous of *CgPax7*, a preliminary phylogenetic analysis was conducted. All sequences of bivalves were clustered a big clade, Pax7 in *C. gigas* was close to *PpPax3*, supporting in high homology with *PpPax3*, because Pax3 and Pax7 genes existed in the form of an ancestral gene in

protostomes, ascidians and amphioxus, and then were separated into two genes in vertebrates by duplication of the ancestral gene (Akolkar et al., 2016). It was speculated that the structural and functional similarity and diversity of Pax7 with Pax3 in bivalves.

Knowledge of spatio-temporal expression patterns of a given gene is valuable for assigning its function. In present study, during the embryonal developmental stages, *CgPax7* transcript level was significantly increased at D-shaped larval 2 stage and it was clearly observed on margins of the growing valve area that will form the mantle, which is in direct contact with the environment and has a sensory function as well as secret biomineralization proteins to form the shell (Ding et al., 2015). In adult oyster, *CgPax7* was ubiquitously expressed in mantle edge, central mantle, gill, labial lap, adductor muscle and digestive gland examined, indicating the expression of *CgPax7* gene was no tissues specificity, maybe related to functional diversity of Pax7 gene in *C. gigas*.

4.2. The role of *CgPax7* in melanin synthesis

RNAi is a powerful method to inhibit specific gene expression. Here, no matter in larval and adult oysters, feeding *CgPax7* dsRNA resulted in significant low expression of *CgPax7*, demonstrating achievement of very effective RNAi in *C. gigas*. The defects in melanosome structure were observed in *CgPax7* knockdown oysters. Similar melanosome defects and disruption of melanosome integrity have also been observed in zebra fish (Braasch et al., 2009), brown mice (Moyer, 1966) and human OCA3 patients (Kidson et al., 1993). TYRP1 participate in the melanogenic complex on the internal surface of the melanosomal membrane (Kobayashi and Hearing, 2007), so it was hypothesized that Pax7 maybe influence melanosome structure by regulating Tyrp1. In addition, between *CgPax7* silencing and control group, tyrosinase activity detection and histology evidence indicated that *CgPax7* play a vital role in melanin synthesis in *C. gigas*. Similarly, in *P. penguin*, Pax3 gene was considered to participate in regulating melanin synthesis by Tyr pathway (Yu et al., 2018b). Roberts et al. (2016) have confirmed that *pax7a*-associated blotch morphs result primarily from modulation of melanophore development and survival. In vertebrate, the importance of Pax3 to the melanocyte population during development is evident by the lack of hair and skin pigmentation in mice and humans with Pax3 gene mutations (Medic and Ziman, 2010). Here we analyzed the influence of Pax7 knockdown on the expression of melanin synthesis-relative genes in *C. gigas*. The data showed that *CgPax7* knockdown caused a significant decrease in *Tyrp1*, *Tyrp2* and *Cdk2* expression and tyrosinase activity, which caused a reduction in melanin synthesis (Braasch et al., 2009), similar to the influence of Tyr silencing (Yu et al., 2018a). Tyr catalyze two initial reaction and is an important rate-limiting enzyme in melanin synthesis (Busca and Ballotti, 2000). In vertebrates, there are other transcription factors involved in regulation in the network. They work, in single factor or complex of factors, such as PAX3, SOX10 and CREB to directly activate the MITF and indirectly regulate the expression of Tyr, *Tyrp1* and *Tyrp2* (Busca and Ballotti, 2000). In present study, there was no significant difference in *CgMitf* mRNA after *CgPax7* knockdown in larval and adult oysters. It was speculated that other factors like SOX10 and CREB also directly activate MITF leading to no significant changes of *Mitf* gene expression. Or MITF was not important regulation factor in melanin synthesis in *C. gigas*, which is needed to be further studied. Moreover, Tyr expression was significantly downregulated in larval stage while was significantly upregulated in mantle of adult oyster after *CgPax7* knockdown. *CgPax7* silencing led to an obvious increase in *CgTyr* expression. A possible explanation for this phenomenon was that the reduction of tyrosinase protein by *CgPax7* silencing might partly damage of normal cells functions, because tyrosinase involved in several important physiological processes including pigment synthesis, oxygen transport, innate immunity and wound healing (Cerenius et al., 2008). The cell damage led to the up-regulation of *CgTyr* through another pathway. Except Tyr, the other two members of tyrosinase gene family, *Tyrp1* and *Tyrp2* also was examined that exhibit the lower expression

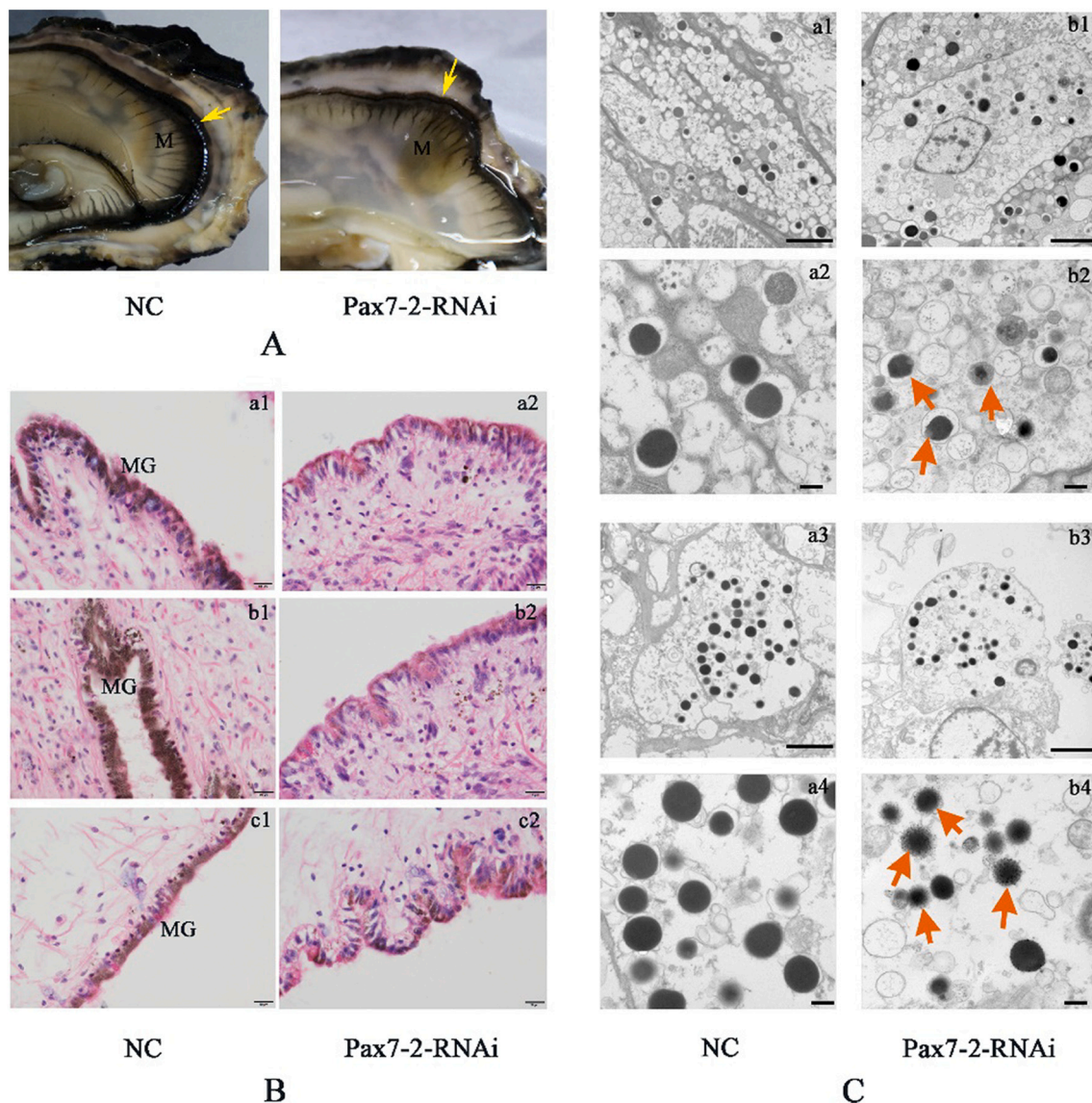


Fig. 6. Mantle morphology in control and *CgPax7* silencing groups. A. The mantle edge pigmentation of *C. gigas*. The mantle edge was shown with yellow arrows. The result showed 1000 \times magnifications with scale bars equaling 10 μ m. B. Histochemistry of mantle edge in *C. gigas*. a1 - c1 indicated the control group, a2 - b2 meant the *CgPax7-2* silencing group. C. Ultrastructure of mantle edge in *C. gigas*. a1 - a4 indicated the control group, b1 - b4 meant the *CgPax7-2* silencing group. Upper rows showed 15,000 \times , lower rows 30,000 \times magnifications with scale bars equaling 2 μ m and 0.5 μ m, respectively. M: mantle; MG: melanin granules. (For interpretation of the references to color in this figure legend, the reader is referred to the web version of this article.)

level after *CgPax7-2* silencing, which is possible to effect melanosome formation. Previous study found that simultaneous knockdown of both *Tyrp1* genes results in severe melanosome defects (Braasch et al., 2009). Melanosome defects were also detected in our TEM results, suggesting that *Pax7* maybe influence melanosome structure by regulating *Tyrp1*. Furthermore, *CgPax7* silencing obviously decreased the *CgCdk2* expression, because *Cdk2* was important gene in melanocyte proliferation in mammals.

In general, these findings showed that less melanin accompanied by severe melanosome defects after *CgPax7-2* knockdown. Less melanin was synthesized in *CgPax7-2* silencing group may be caused by the co-action of these key downstream genes related to melanin, such as *Tyr*, *Tyrp1*, *Tyrp2* and *Cdk2*. It was suspected that *CgPax7* play an important regulating role in melanin synthesis by Tyr pathway in *C. gigas*. A *Pax3-Mitf-tyr* axis was supposed by functional analysis in *P. penguin* (Yu et al., 2018b), whether there are the same regulatory mechanisms and MITF work as a member in *C. gigas* still needs a lot of research in the future.

5. Conclusion

Here, *CgPax7* was significantly expressed in mantle at D-shaped 2 stage and ubiquitously expressed in six examined tissues. The *CgPax7* silencing significantly inhibited the transcriptions of *CgPax7*, *CgTyr*, *CgTyrip1*, *CgTyrip2* and *CgCdk2*, genes involved in Tyr-mediated melanin synthesis, but had no effect on *CgMitf* and an increased effect on *CgTyr* in adult oyster. Furthermore, melanosome defects, tyrosinase activity and melanin granules were diminished as the result of *CgPax7* silencing. Overall, this is the first report of *Pax7* knockdown using RNAi which not only produced significant reduction in mRNA and melanin levels but it also resulted in a morphological change of melanosomes. The results demonstrated that *CgPax7* play a crucial role in melanin synthesis by indirectly regulating the expression of *Tyr* in *C. gigas*. The *Pax7-Tyr-melanin* axis was considered a potential strategy in melanin synthesis of *C. gigas*.

Declaration of Competing Interest

The authors declare that they have no known competing financial interests or personal relationships that could have appeared to influence the work reported in this paper.

Acknowledgments

This work was supported by the grants from National Natural Science Foundation of China (31972789), Earmarked Fund for Agriculture Seed Improvement Project of Shandong Province (2020LZGC016), and Industrial Development Project of Qingdao City (20-3-4-16-nsh).

Appendix A. Supplementary data

Supplementary data to this article can be found online at <https://doi.org/10.1016/j.cbpb.2022.110720>.

References

- Akolkar, D.B., Asaduzzaman, M., Kinoshita, S., Asakawa, S., Watabe, S., 2016. Characterization of Pax3 and Pax7 genes and their expression of patterns during different development and growth stages of Japanese pufferfish *Takifugu rubripes*. *Gene* 575, 21–28. <https://doi.org/10.1016/j.gene.2015.08.031>.
- Bian, C., Li, R.H., Wen, Z.Y., Ge, W., Shi, Q., 2021. Phylogenetic analysis of core melanin synthesis genes provides novel insights into the molecular basis of albinism in fish. *Front. Genet.* 12, 707228 <https://doi.org/10.3389/fgene.2021.707228>.
- Blake, J., Ziman, R., 2014. Pax genes: regulators of lineage specification and progenitor cell maintenance. *Development* 141, 737–751. <https://doi.org/10.1242/dev.091785>.
- Braasch, I., Daniel, L., Volff, J.N., Schartl, M., 2009. Pigmentary function and evolution of tyrp1 gene duplicates in fish. *Pigment Cell Melanoma. Res.* 22, 839–850. <https://doi.org/10.1111/j.1755-148X.2009.00614.x>.
- Busca, R., Ballotti, R., 2000. Cyclic AMP a key messenger in the regulation of skin pigmentation. *Pigment Cell Res.* 13, 60–69. <https://doi.org/10.1034/j.1600-0749.2000.130203.x>.
- Cerenius, L., Lee, B.L., Söderhäll, K., 2008. The proPO-system: pros and cons for its role in invertebrate immunity. *Trends Immunol.* 29, 263–271. <https://doi.org/10.1016/j.it.2008.02.009>.
- Choi, S.H., Jee, B.Y., Lee, S.J., Kim, J.W., Jeong, H.D., Kim, K.H., 2013. Effects of RNA interference mediated knock-down of hypoxia-inducible factor- α on respiratory burst activity of the Pacific oyster *Crassostrea gigas* hemocytes. *Fish Shellfish Immunol.* 35, 476–479. <https://doi.org/10.1016/j.fsi.2013.05.001>.
- Del Marmol, V., Beermann, F., 1996. Tyrosinase and related proteins in mammalian pigmentation. *FEBS Lett.* 381, 165–168. [https://doi.org/10.1016/0014-5793\(96\)00109-3](https://doi.org/10.1016/0014-5793(96)00109-3).
- Ding, J., Zhao, L., Chang, Y.Q., Zhao, W.M., Du, Z.L., Hao, Z.L., 2015. Transcriptome sequencing and characterization of Japanese scallop *Patinopekten yessoensis* from different shell color lines. *PLoS One* 10, e0116406. <https://doi.org/10.1371/journal.pone.0116406>.
- Du, Y., Zhang, L.L., Xu, F., Huang, B.Y., Zhang, G.F., Li, L., 2013. Validation of housekeeping genes as internal controls for studying gene expression during Pacific oyster (*Crassostrea gigas*) development by quantitative real-time PCR. *Fish Shellfish Immunol.* 34, 939–945. <https://doi.org/10.1016/j.fsi.2012.12.007>.
- Fabioux, C., Corporeau, C., Quillien, V., Favrel, P., Huvet, A., 2009. In vivo RNA interference in oyster –vasa silencing inhibits germ cell development. *FEBS J.* 276, 2566–2573. <https://doi.org/10.1111/j.1742-4658.2009.06982.x>.
- Fang, D., Kute, T., Setaluri, V., 2001. Regulation of tyrosinase-related protein-2 (TYRP2) in human melanocytes: relationship to growth and morphology. *Pigment Cell Res.* 14, 132–139. <https://doi.org/10.1034/j.1600-0749.2001.140209.x>.
- Fang, W.Y., Huang, J.R., Li, S.Z., Lu, J.G., 2022. Identification of pigment genes (melanin, carotenoid and pteridine) associated with skin color variant in red tilapia using transcriptome analysis. *Aquaculture* 547, 737429. <https://doi.org/10.1016/j.aquaculture.2021.737429>.
- Feng, D.D., Li, Q., Yu, H., 2019. RNA interference by ingested dsRNA-expressing bacteria to study shell biosynthesis and pigmentation in *Crassostrea gigas*. *Mar. Biotechnol.* 21, 526–536. <https://doi.org/10.1007/s10126-019-09900-2>.
- Hartman, M.L., Czyz, M., 2015. MITF in melanoma: mechanisms behind its expression and activity. *Cell. Mol. Life Sci.* 72, 1249–1260. <https://doi.org/10.1007/s00018-014-1791-0>.
- Hayashi, S., Drayton, B., Aurade, F., Rocancourt, D., Buckingham, M., Relaix, F., 2010. Conserved functions of PAX3/7 during evolution. *Dev. Biol.* 344, 528–529. <https://doi.org/10.1016/j.ydbio.2010.05.386>.
- Hu, B.Y., Li, Q., Yu, H., 2021. RNA interference by ingested dsrna-expressing bacteria to study porphyrin pigmentation in *Crassostrea gigas*. *Int. J. Mol. Sci.* 22, 6120. <https://doi.org/10.3390/ijms22116120>.
- Huan, P., Wang, H.X., Liu, B.Z., 2016. Assessment of housekeeping genes as internal references in quantitative expression analysis during early development of oyster. *Genes Genet. Syst.* 91, 257–265. <https://doi.org/10.1266/ggs.16-00007>.
- Huvet, A., Fleury, E., Corporeau, C., Quillien, V., Daniel, J.Y., Riviere, G., Boudry, P., Fabioux, C., 2012. In vivo RNA interference of a gonad-specific transforming growth factor- β in the pacific oyster *Crassostrea gigas*. *Mar. Biotechnol.* 14, 402–410. <https://doi.org/10.1007/s10126-011-9421-4>.
- Huvet, A., Béguel, J.-P., Cavaleiro, N.P., Thomas, Y., Quillien, V., Boudry, P., Alunno-Bruscia, M., Fabioux, C., 2015. Disruption of amylase genes by RNA interference affects reproduction in the Pacific oyster *Crassostrea gigas*. *J. Exp. Biol.* 218, 1740–1747. <https://doi.org/10.1242/jeb.116699>.
- Ipsaro, J.J., Joshua-Tor, L., 2015. From guide to target: molecular insights into eukaryotic RNA-interference machinery. *Nat. Struct. Mol. Biol.* 22, 20–28. <https://doi.org/10.1038/nsmb.2931>.
- Ito, S., Wakamatsu, K., Glass, K., Simon, J.D., 2013. High-performance liquid chromatography estimation of cross-linking of dihydroxyindole moiety in eumelanin. *Anal. Biochem.* 434, 221–225. <https://doi.org/10.1016/j.ab.2012.12.005>.
- Kidson, S.H., Richards, P.D., Rawoot, F., Kromberg, J.G., 1993. An ultrastructural study of melanocytes and melanosomes in the skin and hair bulbs of rufous albinos. *Pigment Cell Res.* 6, 209–214. <https://doi.org/10.1111/j.1600-0749.1993.tb00604.x>.
- Kobayashi, T., Hearing, V.J., 2007. Direct interaction of tyrosinase with Tyrp1 to form heterodimeric complexes in vivo. *J. Cell Sci.* 120, 4261–4268. <https://doi.org/10.1242/jcs.017913>.
- Land, E.J., Ramsden, C.A., Riley, P.A., 2004. Quinone chemistry and melanogenesis. *Methods Enzymol.* 378, 88–109. [https://doi.org/10.1016/S0076-6879\(04\)78005-2](https://doi.org/10.1016/S0076-6879(04)78005-2).
- Lang, D., Lu, M.M., Huang, L., Engleka, K.A., Zhang, M., Chu, E.Y., Lipner, S., Skoultschi, A., Millar, S.E., Epstein, J.A., 2005. Pax3 functions at a nodal point in melanocyte stem cell differentiation. *Nature* 433, 884–887. <https://doi.org/10.1038/nature03292>.
- Lang, D., Powell, S.K., Plummer, R.S., Young, K.P., Ruggeri, B.A., 2007. PAX genes: roles in development, pathophysiology, and cancer. *Biochem. Pharmacol.* 73, 1–14. <https://doi.org/10.1016/j.bcp.2006.06.024>.
- Lee, D.H., Ahn, S.S., Kim, J.B., Lim, Y., Lee, Y.H., Shin, S.Y., 2018. Downregulation of α -melanocyte-stimulating hormone-induced activation of the Pax3-MITF-Tyrosinase axis by sorghum ethanolic extract in B16F10 melanoma cells. *Int. J. Mol. Sci.* 19, 1640. <https://doi.org/10.3390/ijms19061640>.
- Livak, K.J., Schmittgen, T.D., 2001. Analysis of relative gene expression data using real-time quantitative PCR and the 2(T) (-Delta Delta C) method. *Methods* 25, 402–408. <https://doi.org/10.1006/meth.2001.1262>.
- Medic, S., Ziman, M., 2010. PAX3 expression in normal skin melanocytes and melanocytic lesions (Naevi and Melanomas). *PLoS One* 5, e9977. <https://doi.org/10.1371/journal.pone.0009977>.
- Moyer, F.H., 1966. Genetic variations in the fine structure and ontogeny of mouse melanin granules. *Am. Zool.* 6, 43–66. <https://doi.org/10.1093/icb/6.1.43>.
- Navet, S., Buresi, A., Baratte, S., Andouche, A., Bonnaud-Ponticelli, L., Bassaglia, Y., 2017. The Pax gene family: highlights from cephalopods. *PLoS One* 12, e0172719. <https://doi.org/10.1371/journal.pone.0172719>.
- Nord, H., Deonhag, N., Muck, J., von Hofsten, J., 2016. Pax7 is required for establishment of the xanthophore lineage in zebrafish embryos. *Mol. Biol. Cell* 27, 1853–1862. <https://doi.org/10.1091/mbc.e15-12-0821>.
- Payton, L., Perrigault, M., Bourdineaud, J.-P., Marcel, A., Massabuau, J.-C., Tran, D., 2017. Trojan horse strategy for non-invasive interference of clock gene in the oyster *Crassostrea gigas*. *Mar. Biotechnol.* 19, 361–371. <https://doi.org/10.1007/s10126-017-9761-9>.
- Reynolds, E.S., 1963. The use of lead citrate at high pH as an electron opaque stain in electron microscopy. *J. Cell Biol.* 17, 208–212. <https://doi.org/10.1083/jcb.17.1.208>.
- Roberts, R.B., Moore, E.C., Kocher, T.D., 2016. An allelic series at pax7a is associated with colour polymorphism diversity in Lake Malawi cichlid fish. *Mol. Ecol.* 26, 2625–2639. <https://doi.org/10.1111/mec.13975>.
- Ruska, A.B., Alfaro, A.C., Young, T., Watts, E., Adams, S.L., 2020. Development stage of cryopreserved mussel (*Perna canaliculus*) larvae influences post-thaw impact on shell formation, organogenesis, neurogenesis, feeding ability and survival. *Cryobiology* 93, 121–132. <https://doi.org/10.1016/j.cryobiol.2020.01.021>.
- Saenko, S., Schilthuisen, M., 2021. Evo-devo of shell colour in gastropods and bivalves. *Curr. Opin. Genet. Dev.* 69, 1–5. <https://doi.org/10.1016/j.cde.2020.11.009>.
- Schallreuter, K.U., Kothari, S., Chavan, B., Spencer, J.D., 2008. Regulation of melanogenesis—controversies and new concepts. *Exp. Dermatol.* 17, 395–404. <https://doi.org/10.1111/j.1600-0625.2007.00675.x>.
- Scherholz, M., Redl, E., Wollesen, T., De Oliveira, A.L., Todt, C., Wanninger, A., 2017. Ancestral and novel roles of Pax family genes in mollusks. *BMC Evol. Biol.* 17, 81. <https://doi.org/10.1186/s12862-017-0919-x>.
- Takgi, R., Miyashita, T., 2014. A cDNA cloning of a novel alpha-class tyrosinase of *Pinctada fucata*: its expression analysis and characterization of the expressed protein. *Enzym. Res.* 2014, 1–9. <https://doi.org/10.1155/2014/780549>.
- Wang, J.M., Xue, R.P., Chen, Q., Zhan, P.P., Han, Q.X., Peng, R.B., Jiang, X.M., 2020. Histology and ultrastructure of ink gland and melanogenesis in the cuttlefish *Sepia pharaonica*. *Invertebr. Biol.* 139, e12306 <https://doi.org/10.1111/ivb.12306>.
- Yang, B.Y., Qin, J., Shi, B., Han, G.D., Chen, J., Huang, H.Q., Ke, C.H., 2012. Molecular characterization and functional analysis of adrenergic like receptor during larval metamorphosis in *Crassostrea angulata*. *Aquaculture* 366–367, 54–61. <https://doi.org/10.1016/j.aquaculture.2012.08.040>.
- Yao, H.H., Cui, B.Y., Li, X.Y., Lin, Z.H., Dong, Y.H., 2020. Characteristics of a novel tyrosinase gene involved in the formation of shell color in hard clam *Meretrix meretrix*. *J. Ocean Univ. China* 19, 183–190. <https://doi.org/10.1007/s11802-020-4202-1>.

- Yu, F.F., Pan, Z.N., Qu, B.L., Yu, X.Y., Xu, K.H., Deng, Y.W., Liang, F.L., 2018a. Identification of a tyrosinase gene and its functional analysis in melaninsynthesis of *Pteria penguin*. *Gene* 656, 1–8. <https://doi.org/10.1016/j.gene.2018.02.060>.
- Yu, F.F., Qu, B.L., Lin, D.D., Deng, Y.W., Huang, R.L., Zhong, Z.M., 2018b. Pax3 gene regulated melanin synthesis by tyrosinase pathway in *Pteria penguin*. *Int. J. Mol. Sci.* 19, 3700. <https://doi.org/10.3390/ijms19123700>.
- Zhang, S.J., Wang, H.X., Yu, J.J., Jiang, F.J., Yue, X., Liu, B.Z., 2018. Identification of a gene encoding microphthalmia-associated transcription factor and its association with shell color in the clam *Memetrix petechialis*. *Comp. Biochem. Physiol. B Biochem. Mol. Biol.* 225, 75–83. <https://doi.org/10.1016/j.cbpb.2018.04.007>.
- Zhu, Y.J., Li, Q., Yu, H., Liu, S.K., Kong, L.F., 2021. Shell biosynthesis and pigmentation as revealed by the expression of tyrosinase and tyrosinase-like protein genes in Pacific oyster (*Crassostrea gigas*) with different shell colors. *Mar. Biotechnol.* <https://doi.org/10.1007/s10126-021-10063-2>.